OPTOELECTRONICS AND ADVANCED MATERIALS – RAPID COMMUNICATIONS Vol. 14, No. 9-10, September-October 2020, p. 399 - 409

# Diversity and absolute combining time domain transmitter for enhanced asymmetrically and symmetrically clipped optical OFDM (EASCO-OFDM)

A. F. ABAS*, M. S. BAIG, M. T. ALRESHEEDI, H. VETTIKALLADI, M. ABDEL-RAHMAN
*Department of Electrical Engineering, College of Engineering, P.O. Box 800, King Saud University, Riyadh 11421, Kingdom of Saudi Arabia*

This paper presents a novel diversity and absolute combining time domain transmitter (DACTDT) for the Enhanced Asymmetrically and Symmetrically Clipped Optical (EASCO) OFDM system. This system estimates and eliminates the clipping distortion of the signal at the transmitter. The spectral efficiency and bit-error-rate (BER) were improved. The DACTDT effectively combines time domain diversity combining technique (TDDT)-applied to ACO-OFDM stream and the novel absolute combining time domain technique (ACTDT)-applied to ESCO-OFDM stream. Both TDDT and the proposed ACTDT utilize the clipping distortion of their respective streams to improve their performance. In terms of Optical Signal-to-Noise Ratio (OSNR), at a BER of $10^{-3}$ with 1024-QAM, the proposed EASCO-DACTDT OFDM performs 8.3 dB better than EASCO-OFDM.

(Received December 18, 2019; accepted October 21, 2020)

*Keywords*: Clipping distortion, Diversity combining technique, ACO-OFDM, ESCO-OFDM

## 1. Introduction

Optical Orthogonal Frequency Division Multiplexing (OOFDM) with Intensity Modulation/Direct Detection (IM/DD) is preferred in optical wireless systems. By implementing IM/DD rather than coherent receiver systems, the structure of the receiver systems is simplified, reducing the number of components and the system complexity. In this system, the OFDM signals, which are bipolar and complex, have to be converted to real and non-negative unipolar signals [1-3]. This process is important to assure that the OFDM signal can be detected by the IM/DD receiver, which only recognizes the non-negative unipolar signals. In recent years, many such systems were proposed namely DC-biased Optical OFDM (DCO-OFDM) [2, 4-8], Asymmetrically-Clipped Optical OFDM (ACO- OFDM) [3,[1] 5-8] and Unipolar OFDM (U-OFDM) [9], which is also known as U/Flip-OFDM in [10].

Among those systems, ACO-OFDM is highly power efficient, therefore, became the system of interest. Developed around ACO-OFDM, many techniques have been proposed namely Asymmetrically Clipped DC biased optical OFDM (ADO-OFDM) [3, 6], Hybrid ACO-OFDM (HACO-OFDM) [2] , Asymmetrically and Symmetrically Clipped Optical OFDM (ASCO-OFDM) [5, 7, 9] and Layered/Enhanced ACO-OFDM [3, 4]. In this work the proposed systems are developed based on ASCO-OFDM system.

ASCO-OFDM is a system that combines ACO-OFDM carried over its odd subcarrier, and Symmetrically Clipped Optical OFDM (SCO-OFDM) on the even subcarriers. In this system, clipping distortion of both ACO-OFDM and SCO-OFDM affects the data on the even subcarriers. The clipping distortion of ACO-OFDM that is estimated from the received ACO-OFDM signal is subtracted from the even subcarriers. The SCO-OFDM clipping distortion is subtracted by the complex processing technique of U/Flip-OFDM at the receiver. This technique compensates for the loss of information due to clipping at even subcarriers due to even symmetry.

ASCO-OFDM increases the overall system's architecture complexity. On the other hand, it has better performances in terms of symbol error rate (SER) and optical power as compared to ADO-OFDM [5, 6]. To deal with complex system architecture, Spectrally Efficient ASCO-OFDM (SEASCO-OFDM) technique [7] was developed. In this technique, the loss of information (through clipping on SCO-OFDM signal) is recovered by using similar techniques to [8]. In this paper, the technique is referred to as Enhanced SCO (ESCO)-OFDM.

Another important issue is the clipping distortion of ACO-OFDM. This distortion occurs on the even subcarriers, and normally discarded. However, it carries 50% of the transmitted signal power [9], and therefore, cannot be simply ignored. Hence, to effectively utilize it, a new receiver, which uses the Diversity Combining (DC) technique was introduced for ACO-OFDM [9, 10]. The same technique was later applied to ASCO-OFDM [11], which enhanced its performance. Another application of the same technique was reported in [12]. In the mentioned techniques, DC was applied in the receiver after the equalization process, which require the use of additional Fourier Frequency Transform (FFT)s to process the non-linear operations. Recently, a new technique was proposed that uses diversity combining via symmetry recovering

technique to reduce the complex operation of Inverse FFT (IFFT) [13].

In this paper, the extension of SEASCO-OFDM system [7] is presented with the aim to

1) Estimate and eliminate the Clipping distortion in ESCO-OFDM transmitter
2) Utilize the clipping distortion to enhance the transmitter output
3) Reduce the number of complex multiplications of the IFFT/FFT operations at the receiver

## 2. Estimation and Elimination of the Clipping distortion in ESCO-OFDM transmitter

There are two main issues that arise due to direct clipping at even subcarriers, which affect the system performance. The first issue is the loss of information due to symmetry. The second issue is the clipping distortion that interferes with the data information on the even subcarriers, which affects data recovery process. To deal with the mentioned issues, a proposed method named as EASCO-OFDM is presented in this section.

### 2.1. System modeling

Fig. 1 (a) and (b) respectively shows the block diagram of the proposed EASCO-OFDM transmitter and receiver. From Fig. 1(a), it is shown that in the first step, the data (Data in) are passed through a serial to parallel (S/P) converter. Then, mapped using QAM Modulator that is constrained with a Hermitian symmetry. This process results in a complex data signal X that is divided into odd and even streams, which are input into the two blocks of N-point IFFT respectively that generate real valued signals.

The odd stream signal $X_{odd}$, which carries the data on the N/4 of the odd subcarriers is represented as

$$X_{odd} = \begin{bmatrix} 0, X_1, 0, X_3, 0, \dots, X_{\frac{N}{2}-1}, 0, X_{\frac{N}{2}-1}{}^{*}, \dots \\ \dots, X_3{}^{*}, 0, X_1{}^{*}, 0 \end{bmatrix} \quad (1)$$

where 'N' is the total number of subcarriers.

The real valued $x_{odd}$ is clipped to generate ACO-OFDM signal $x_{ACO}$ given as

$$x_{ACO} = \frac{1}{2}(x_{odd} + |x_{odd}|) \quad (2)$$

$$= x_{ACO\_odd} + x_{ACO\_even} \quad (3)$$

where $x_{ACO\_odd}$ represent the odd subcarriers of the ACO-OFDM signal $x_{ACO}$ that contains the data $(0.5(x_{odd}))$ . On the other hand, $x_{ACO\_even}$ represent the even subcarrier s of the ACO-OFDM signal $x_{ACO}$ containing the clipping distortion$(0.5(|x_{odd}|))$.

The even stream $X_{even}$ carrying the data on the N/4 of subcarriers is represented as

$$X_{even} = \begin{bmatrix} 0,0, X_2, \dots, X_{\frac{N}{2}-2}, 0, X_{\frac{N}{2}-2}{}^{*}, \\ \dots . X_2{}^{*}, 0,0 \end{bmatrix} \quad (4)$$

where $X_0$ and $X_{N/2}$ are set to zero.

Clipping of real valued signal $x_{even}$ (Eq. 4) results in loss of information. This is due to even symmetry at the even subcarriers [14]. To compensate for this loss of information, the $x_{even,n}$ is split across the symmetry in two frames in which frame 1 (from 0 to N/2-1) is negatively clipped to zero represented as $x_{even,n}^{f1} = 0.5\,(x_{even,n}^{f1} + |x_{even,n}^{f1}|)$, and an absolute of positive clipping is carried on frame 2 (from N/2 to N-1), which is represented as $x_{even,n}^{f2} = 0.5(-x_{even,n}^{f2} + |x_{even,n}^{f2}|)$, and is non- negative as in [14]. This process results in the newly generated non-negative ESCO-OFDM signal and is mathematically expressed as

$$x_{ESCO,n} = \begin{cases} x_{even,n}^{f1}\ , & 0 < \mathrm{n} < \frac{\mathrm{N}}{2} - 1 \\ x_{even,n}^{f2}\ , & \frac{\mathrm{N}}{2} < \mathrm{n} + \frac{\mathrm{N}}{2} < \mathrm{N} - 1 \end{cases} \quad (5)$$

$$x_{ESCO,n} = \frac{1}{2}\begin{cases} (x_{even,n}^{f1} + |x_{even,n}^{f1}|)\,, & 0 < n < \frac{N}{2} - 1 \\ (-x_{even,n}^{f2} + |x_{even,n}^{f2}|), & \frac{N}{2} < n + \frac{N}{2} < N - 1 \end{cases} \quad (6)$$

Eq (6) can also be expressed as

$$x_{ESCO,n} = \frac{1}{2}(x_{ESCO\_D} + c_{ESCO}) \quad (7)$$

where $x_{ESCO\_D}$ represents the positive data on the even subcarriers across the symmetry $n$, which is expressed as

$$x_{ESCO\_D} = \begin{cases} x_{even,n}^{f1}, & 0 < \mathrm{n} < \frac{\mathrm{N}}{2} - 1 \\ -x_{even,n}^{f2}, & \frac{\mathrm{N}}{2} < \mathrm{n} + \frac{\mathrm{N}}{2} < \mathrm{N} - 1 \end{cases} \quad (8)$$

The clipping distortion $c_{ESCO}$, falling on the even subcarriers as a result of clipping, is represented as the absolute value of Eq. (7) as in [12, 14]

$$C_{ESCO} = \begin{cases} |x_{even,n}^{f1}|, & 0 < \mathrm{n} < \frac{\mathrm{N}}{2} - 1 \\ |-x_{even,n}^{f2}|, & \frac{\mathrm{N}}{2} < \mathrm{n} + \frac{\mathrm{N}}{2} < \mathrm{N} - 1 \end{cases} \quad (9)$$

The clipping distortion that is estimated from $x_{even}$ is represented as

$$\widetilde{C_{ESCO}} \approx \begin{cases} \widetilde{C_{ESCO,n}^{f1}} = |x_{even,n}^{f1}|\,, & 0 < \mathrm{n} < \frac{\mathrm{N}}{2} - 1 \\ \widetilde{C_{ESCO,n}^{|f2|}} = |x_{even,n}^{f2}|, & \frac{\mathrm{N}}{2} < \mathrm{n} + \frac{\mathrm{N}}{2} < \mathrm{N} - 1 \end{cases} \quad (10)$$

Eq. (10) is subtracted/cancelled from Eq. (6) to yield $x_{ESCO=}x_{ESCO\_D}$ , i.e. only the data on the even subcarriers. The EASCO-OFDM signal is obtained by combining the generated ACO-OFDM and ESCO-OFDM signals in Eq. (3) and (7) respectively to obtain the resulting signal shown in Fig.1 (a), which can be represented as

$$x_{EASCO} = x_{ACO} + x_{ESCO} \tag{11}$$

Cyclic Prefix (CP) is appended to this signal and converted from parallel to serial (P/S) and digital to analog (D/A). This is followed by the modulation process. The signal is then transmitted over the transmission line represented as $x'_{EASCO}$.

At the Receiver (Fig. 1(b)), the received signal $y'_{EASCO}$ is first converted from an optical to electrical signal using a photodiode and then converted from analog to digital form by using Analog-to-Digital converter (A/D). The shot noise and thermal noise are modelled as additive white Gaussian noise (AWGN) as in [3, 15, 16]. The CP is removed, after the signal is passed through a serial-to-parallel convertor (S/P). The resulting received signal is expressed as

$$y_{EASCO} = x_{EASCO}(n) * h(n) + w(n) \tag{12}$$

where $h(n)$ is the impulse response of the optical channel and $w(n)$ is approximately modelled as additive white Gaussian's noise (AWGN). The received signal is transformed into frequency domain and equalized for the demodulation process. The ACO-OFDM symbols of EASCO-OFDM signals in Eq. (12) are recovered from $Y_{EASCO\_odd}$ (odd subcarriers of received signal $Y_{EASCO}$) as shown in Fig. 1(b). Then, the clipping noise is estimated and removed in time domain to yield ESCO-OFDM symbols $y_{ESCO}$. Following the signal recovery operation, the $Y_{even}$ samples are recovered in frequency domain as shown in Fig. 1(b). In the signal recovery operation, for every zero sample at $0 < n < N/2$, its corresponding information in its inverse form that presents at $\frac{N}{2} < n + \frac{N}{2} < N - 1$ is retrieved. This way, all the clipped information is recovered.

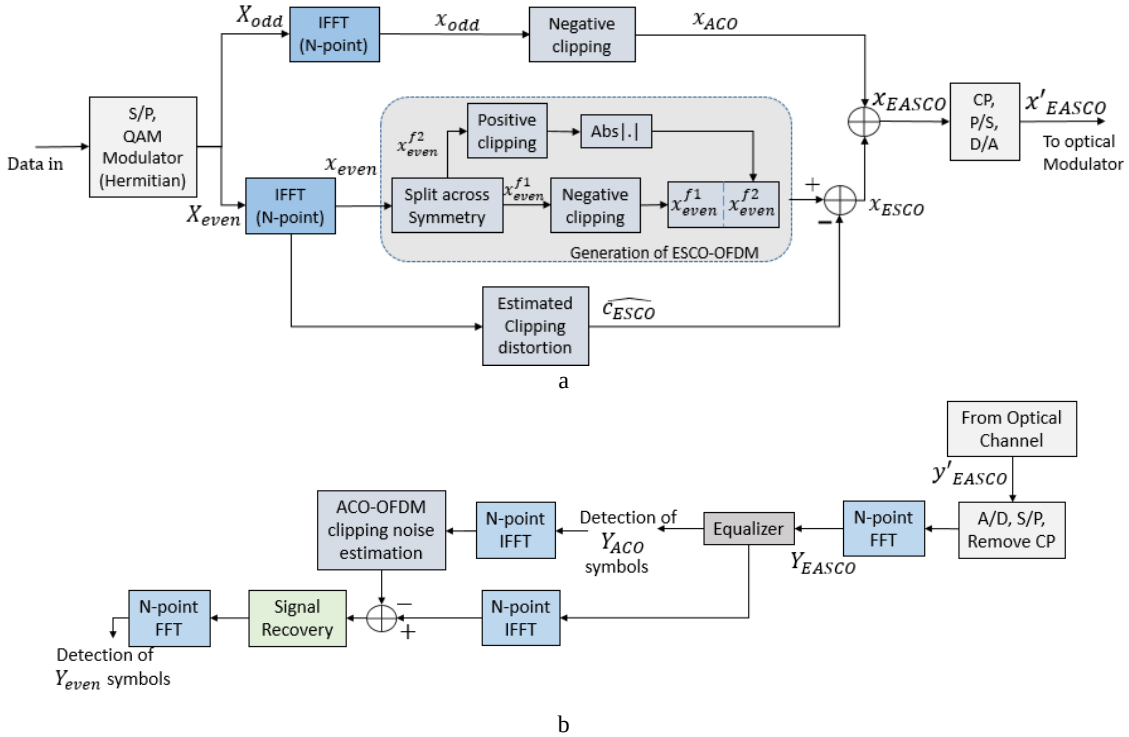


*Fig. 1. Block Diagram of EASCO-OFDM System (a) Transmitter (b) Receiver (color online)*

### 2.2. Performance Evaluation of EASCO-OFDM system

#### *2.2.1. Spectral efficiency*

EASCO-OFDM requires (N/4) and (N/(4-1)) symbol vectors on its odd and even streams respectively. Thus, the spectral efficiency of EASCO-OFDM denoted as $\Im_{EASCO-OFDM}$ in bits/sec/Hz, can be written as

$$\Im_{EASCO-OFDM} = \frac{\left[\left(\frac{N}{4}\right)log_2 M_{ACO} + \left(\frac{N}{4}-1\right)log_2 M_{ESCO}\right]}{N} \tag{13}$$

where $M_{ACO}$ and $M_{ESCO}$ are the size of constellation for ACO-OFDM and ESCO-OFDM respectively. For a large $N$ and same constellation size, Eq.(13) is simplified and approximated as

$$\Im_{EASCO-OFDM} \approx \frac{1}{4}(log_2 M_{ACO} + log_2 M_{ESCO}) \quad (14)$$

ASCO-OFDM requires respectively two $(\frac{N}{4})$ and $(\frac{N}{4}-1)$ symbol vectors on its odd and even streams. Hence, the spectral efficiency, $\Im_{ASCO-OFDM}$ in bits/sec/Hz, of a two frame ASCO-OFDM is given by

$$\Im_{ASCO-OFDM} = \frac{\left[\left(\frac{N}{4}\right)log_2 M_{ACO} + \left(\frac{N}{4}-1\right)\frac{1}{2}log_2 M_{SCO}\right]}{N} \quad (15)$$

where $M_{SCO}$denotes the size of constellation for SCO-OFDM. For a large $N$ and same constellation size, Eq. (15) is simplified and approximated as

$$\Im_{ASCO-OFDM} \approx \frac{1}{4}(log_2 M_{ACO} + \frac{1}{2} log_2 M_{ESCO}) \quad (16)$$

The spectral efficiencies of ASCO-OFDM and EASCO-OFDM in Eq. (14) and (16) respectively for a large $N$ are compared against each other considering the same constellation size and equal optical power for both odd and even subcarriers as listed in Table 1.

*Table 1. Spectral Efficiency Comparison*

| Constellation size groups (same on both odd and even subcarriers) | Spectral Efficiency (bits/sec/Hz) | |
|---|---|---|
| | ASCO-OFDM | EASCO-OFDM |
| 4-QAM | 0.75 | 1 |
| 16-QAM | 1.5 | 2 |
| 64-QAM | 2.25 | 3 |
| 256-QAM | 3 | 4 |
| 1024-QAM | 3.75 | 5 |

From Table 1, it is observed that EASCO-OFDM is 33.33% more spectrally efficient compared to ASCO-OFDM.

### *2.2.2. Computational complexity*

The complexity '$\Theta$' of a system is defined by the number of complex multiplications of IFFT/FFT operations [17]. ASCO-OFDM requires two IFFT's to modulate a conventional ACO-OFDM mapping, and one IFFT to modulate SCO-OFDM mapping at the transmitter. ASCO-OFDM receiver requires two FFT to demodulate the two frames ASCO-OFDM signal, in addition to an IFFT and a FFT to remove the ACO-OFDM clipping distortion. The computational complexity at the transmitter ASCO-OFDM is $3\Theta(Nlog_2 N)$ and at the receiver is $4\Theta(Nlog_2 N)$. In comparison, EASCO-OFDM requires two IFFT's at the transmitter that has a complexity of $2\Theta(Nlog_2 N)$. Its receiver requires one FFT to demodulate the signal and an IFFT and FFT to remove the ACO-OFDM clipping distortion. The complexity at the receiver is $4\Theta(Nlog_2 N)$. Hence, EASCO-OFDM achieves the reduced complexity at the transmitter when compared to ASCO-OFDM system.

### *2.2.3. BER*

The simulation results of the bit error rate (BER) of EASCO-OFDM are presented. For the simulations, the IFFT size 'N' used is 1024, and an oversampling of 4 was used to get accurate results. A total of 256 symbols were used. 128 symbols are mapped from M-QAM constellations ($M \in 4,16,64,256,1024$) to form the input to the IFFT block of the first stream to generate the ACO-OFDM signals. Similarly, the other 127 symbols were used to generate the ESCO-OFDM signal. The optical power is also equally allocated to both odd and even streams. For comparison analysis, the BER simulations are carried for the same spectral efficiency of all the models. The bit error rate BER of EASCO-OFDM is verified with Monte-Carlo simulations as shown in Fig. 2. All simulations were carried for an IFFT size of N=1024 and around 256 symbols were used. The simulations were repeated for 10,000 iterations. As seen from Fig. 2, the theoretical model and Monte-Carlo simulations curves closely match.

The BER performance of EASCO-OFDM is also compared with conventional ASCO-OFDM for same constellation sizes on odd and even subcarriers, which is shown in Fig. 2. For a BER of $10^{-3}$, with 16-QAM, EASCO-OFDM achieves 4.2 dB better SNR than ASCO-OFDM. Interestingly, with 1024-QAM and at the same BER, EASCO-OFDM achieves 4.72 dB better SNR than ASCO-OFDM.

EASCO-OFDM system is successfully presented that has improved performance in terms of spectral efficiency and BER performance in comparison to conventional ASCO-OFDM system. However, in terms of computational complexity, the EASCO-OFDM system achieves reduced complexity only at the transmitter. This is due to the required additional IFFTs at the receiver for accurate estimation and cancellation of ACO-OFDM clipping distortion in time domain. If this clipping distortion is not accurately estimated, it can deteriorate the BER performance of the ESCO-OFDM signal. To resolve this issue, the clipping distortion of ACO-OFDM that contains 50% of the information is utilized by the TDDT technique to enhance the transmitter output which is shown in the next section.

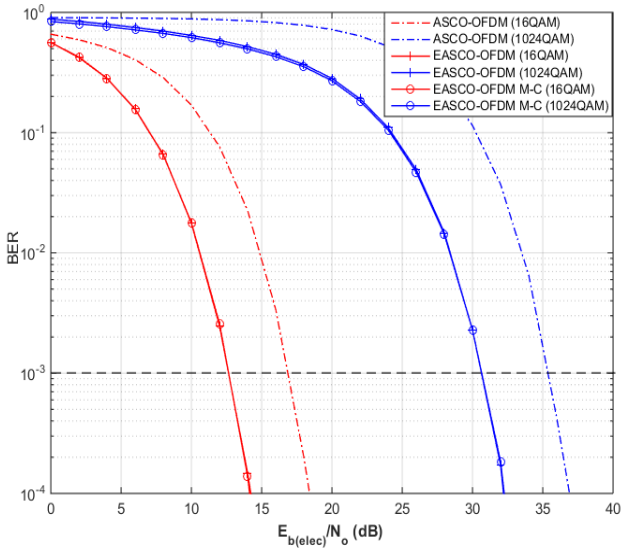


*Fig. 2. BER versus $\frac{E_{b(elec)}}{N_o}$ (dB) for curves of ASCO-OFDM, EASCO-OFDM and EASCO-OFDM M-C (Monte-Carlo) (color online)*

## 3. Utilization of the clipping distortion to enhance the transmitter output

### 3.1. Utilizing Clipping Distortion of ACO-OFDM

To enhance the performance of EASCO-OFDM system, the output of ACO-OFDM signal is input into an ACO-TDDT block at the transmitter as shown in Fig. 3(a). The ACO-TDDT block maximizes the performance by utilizing the clipping distortion of ACO-OFDM signal, which is shown in the following steps. First, the $x^R_{ACO\_even}$ is generated by a non-linear operation in the TDDT block

$$x^R_{ACO\_even} = x_{ACO\_even} * sign(x_{ACO\_odd}) \quad (17)$$

where $x_{ACO\_even}$ represent the even subcarriers of ACO-OFDM signal that contains the clipping distortion. $x_{ACO\_odd}$ represents the odd subcarriers of ACO-OFDM signal. Then, $x^R_{ACO\_even}$ and $x_{ACO\_odd}$ are combined linearly by a weighted sum to obtain an improved estimate that is given as

$$x_{ATDDT} = \alpha * x_{ACO\_odd} + (1-\alpha) * (x^R_{ACO\_even}) \quad (18)$$

where $\alpha$ is the ratio that typically ranges from 0 to 1 and is chosen to maximize the SNR. The EASCO-ATDDT OFDM signal is obtained by combining Eqs. (3) and (7) as shown in Fig. 4 (a) and given as

$$x_{EASCO-ATDDT} = x_{ATDDT} + x_{ESCO} \quad (19)$$

Then CP is appended to signal in Eq. (19). Subsequently the signal is converted from parallel to serial (P/S). This is followed by the modulation process. The signal, represented as $x'_{EASCO-ATDDT}$ is transmitted over the transmission line. At the Receiver (Fig. 3 (b)), the received signal $y'_{EASCO-ATDDT}$ goes through a similar process described in the previous section. The resulting received signal is expressed as

$$y_{EASCO-ATDDT} = x_{EASCO-ATDDT}(n) * h(n) + w(n) \quad (20)$$

This received signal is transformed into frequency domain and equalized for the demodulation process. The ACO-OFDM symbols of EASCO-ATDDT OFDM signals in Eq. (20) are recovered from $Y_{EASCO-ATDDT\_odd}$ (odd subcarriers of received signal $Y_{EASCO-ATDDT}$). The ESCO-OFDM $Y_{ESCO}$ symbols are detected from the $Y_{EASCO-ATDDT\_even}$ (even subcarriers of received signal $Y_{EASCO-ATDDT}$). The $Y_{even}$ symbols are then recovered following the signal recovery operation (as described in Section 2.1). Thus the complexity of the EASCO-ATDDT receiver shown in Fig. 3(b) reduces to $3\Theta(Nlog_2N)$. This shows that utilization of clipping distortion of ACO-OFDM at the transmitter gives an enhanced signal, with the advantage of a reduced complexity at the receiver. However, it is seen that the clipping distortion of ESCO-OFDM is still being eliminated in EASCO-ATDDT. The next section analyses the effect of utilization of the clipping distortion of ESCO-OFDM.

### 3.2. Utilizing clipping distortion for ACO-OFDM and ESCO-OFDM

From the structure shown in Fig. 3, ESCO-TDDT block is introduced as the input to the ESCO-OFDM signal as shown in Fig. 4(a). The signal $x_{ESCO\_D} = (x_{even})$ presents on the even subcarriers. The estimated clipping distortion $\widetilde{c_{ESCO}}$ that is subtracted from Eq. (7) is also fed to the TDDT block. The improved estimate $x_{ESTDDT}$ is obtained similar to Eq. (18) given as

$$x_{ESTDDT} = \alpha * x_{ESCO\_D} + (1-\alpha) * (x^R_{ESCO}) \quad (21)$$

where $x^R_{ESCO}$ is a result of non-linear operation $x^R_{ESCO} = c_{ESCO} * sign(x_{ESCO\_D})$ and '$\alpha$' is chosen to maximize the SNR.

The signals $x_{ATDDT}$ and $x_{ESTDDT}$ are represented by Eqs. (18) and (21) respectively. Both signals are combined to generate EASCO-AESTDDT signal as shown in Eq. (22).

$$x_{EASCO-AESTDDT} = x_{ATDDT} + x_{ESTDDT} \quad (22)$$

Cyclic Prefix (CP) is appended to the resultant signal $x_{EASCO-AESTDDT}$. Then the signal is converted from parallel to serial (P/S). This is followed by the modulation process. The signal is then transmitted over the transmission line represented as $x'_{EASCO-AESTDDT}$. At the Receiver (Fig. 4(b)), the received signal $y'_{EASCO-AESTDDT}$ goes through a similar process described in Section A for

EASCO-OFDM receiver. The output of this process is expressed as

$$y_{EASCO-AESTDDT} = x_{EASCO-AESTDDT}(n) * h(n) + w(n) \quad (23)$$

The enhanced ACO-OFDM (ATDDT) symbols are detected from $Y_{EASCO-AESTDDT\_odd}$ (odd subcarriers of $Y_{EASCO-AESTDDT}$) as shown in Fig. 4(b). Following the signal recovery (as described in Section 2.1), the ESTDDT-OFDM symbols are detected from $Y_{EASCO-AESTDDT\_even}$ (even subcarriers of received signal $Y_{EASCO-AESTDDT}$).

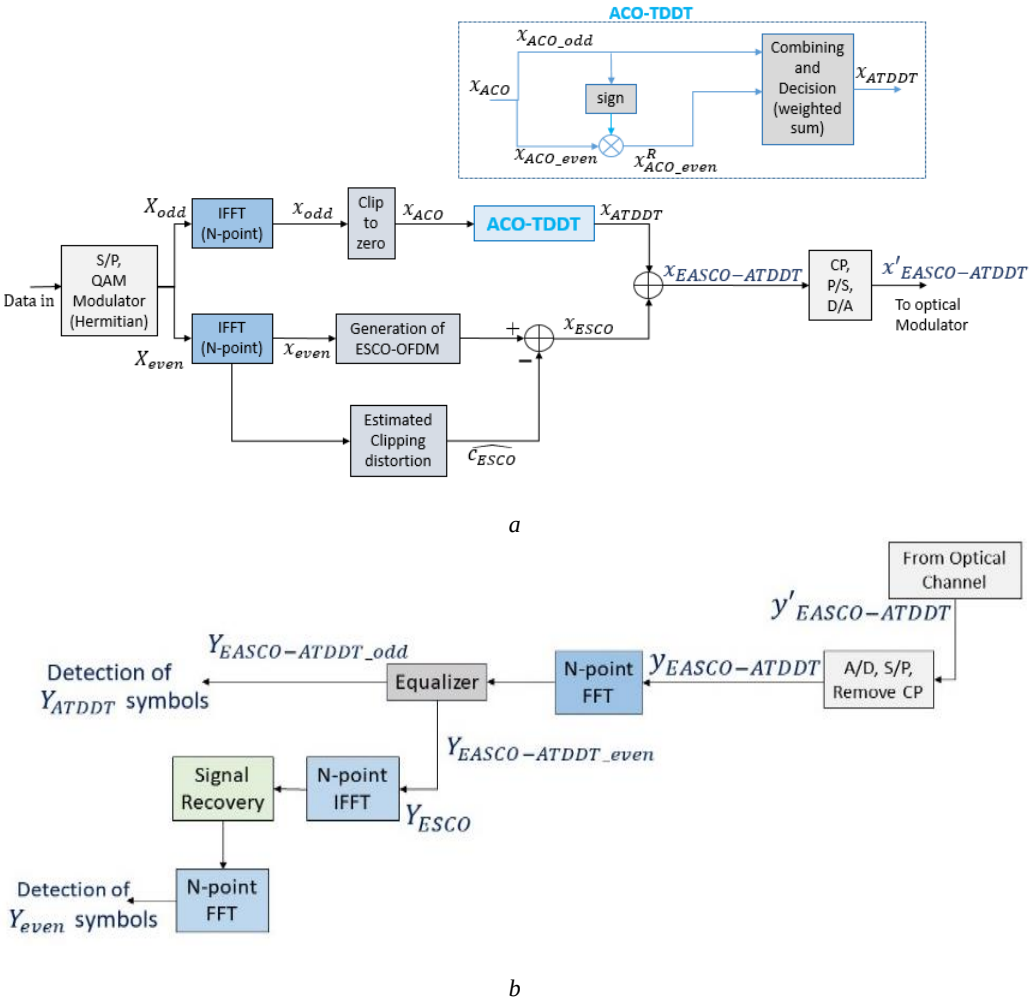


*Fig. 3. Block Diagram of EASCO-ATDDT OFDM System (a) Transmitter (b) Receiver (color online)*

As seen in Fig. 4(b), only one FFT is required to demodulate the enhanced ATDDT whereas for ESTDDT, two IFFT's are needed. So, the computational complexity of the receiver is $3\Theta(Nlog_2N)$. Thus, the EASCO-AESTDDT system generates a signal that produces enhanced ATDDT and ESTDDT signals. However, the complexity of the receiver remains the same in comparison to EASCO-ATDDT (described in the previous section).

The process of generating ESTDDT signal is more complicated than the process of generating ATDDT signal. To generate the ATDDT signal the clipping distortion of ACO-OFDM that are on the even subcarriers can be distinctly combined with the data on odd subcarriers in a non-linear process of TDDT. In contrast, generation of ESTDDT requires the clipping distortion of ESCO-OFDM to interfere with the data on the even subcarriers. This distortion needs to be separated before applying TDDT. The second disadvantage arises when the estimated clipping distortion has to be multiplied by the polarity of the data in a weighted non-linear operation. In the presence of a large noise, the performance of TDDT, which depends on the non-linear operation, gets marginally affected by the sign flipping error [10]. Therefore, it is highly convenient if the estimation of clipping distortion and non-linear operation can be avoided.

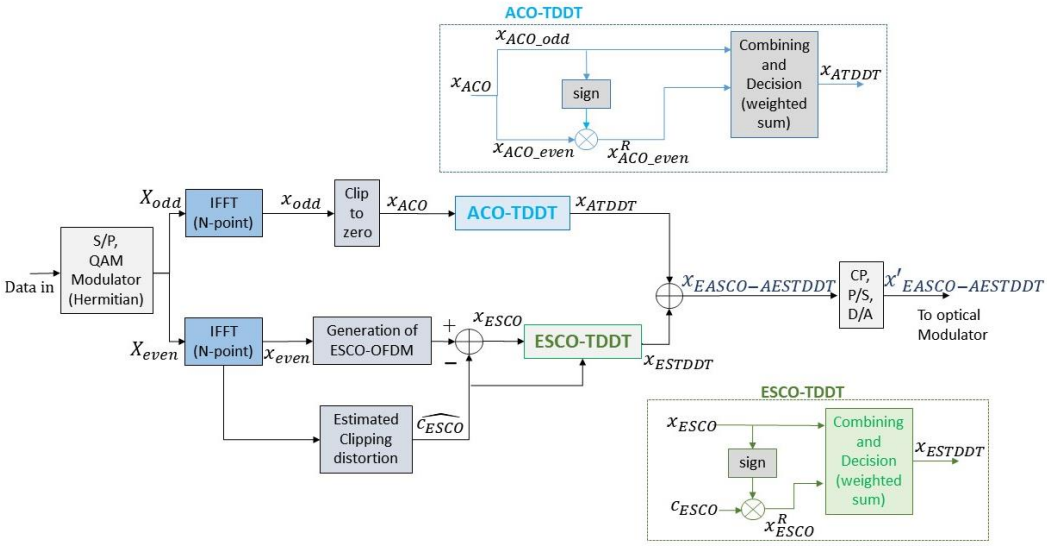


*a*

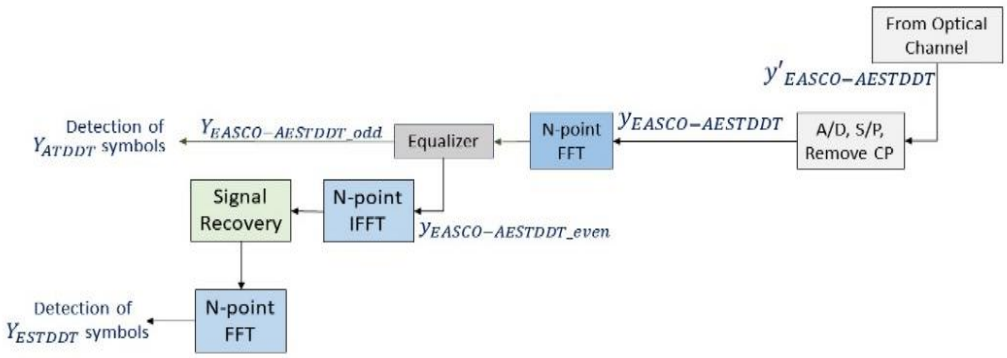


*b*

*Fig. 4. Block Diagram of EASCO-AESTDDT OFDM System (a) Transmitter (b) Receiver (color online)*

### 3.3. Novel method of utilizing clipping distortion without conventional nonlinear process

Fig. 5(a) shows the proposed Absolute Combining Time Domain Technique (ACTDT). The ACTDT block performs the mathematical absolute function (|.|) on the ESCO-OFDM signal to combine the data and the clipping distortion as represented by Eqs. (6) and (7). Thus, both estimation of clipping distortion and the complicated non-linear operation is not required. The EASCO-DACTDT receiver applies pairwise clipping in time domain as in [18] to reduce the effect of noise. The signal $x_{ESCO-ACTDT}$ is detailed as

$$\begin{aligned} x_{ESCO-ACTDT} &\approx |x_{ESCO}| \\ &\approx |\tfrac{1}{2}(x_{ESCO\_D} + c_{ESCO\_D})| \\ &\approx |\tfrac{1}{2}(x_{ESCO\_D} + |x_{ESCO\_D}|)| \end{aligned}$$

$$x_{ESCO-ACTDT} \approx \begin{cases} |\frac{1}{2}(x^{f1}_{even,n} + |x^{f1}_{even,n}|)|, & 0 < n < \frac{N}{2} - 1 \\ |\frac{1}{2}(-x^{f2}_{even,n} + |x^{f2}_{even,n}|)|, & \frac{N}{2} < n + \frac{N}{2} < N - 1 \end{cases}$$

$$x_{ESCO-ACTDT} \approx \begin{cases} \frac{1}{2}\sqrt{\{x^{f1}_{even,n}\}^2 + \{\sqrt{(x^{f1}_{even,n})^2}\}^2}, 0 < n < \frac{N}{2} - 1 \\ \frac{1}{2}\sqrt{\{x^{f2}_{even,n}\}^2 + \{\sqrt{(x^{f2}_{even,n})^2}\}^2}, \frac{N}{2} < n + \frac{N}{2} < N - 1 \end{cases}$$

$$x_{ESCO-ACTDT} \approx \begin{cases} \frac{1}{2}\sqrt{2\{x^{f1}_{even,n}\}^2}, & 0 < n < \frac{N}{2} - 1 \\ \frac{1}{2}\sqrt{2\{x^{f2}_{even,n}\}^2}, & \frac{N}{2} < n + \frac{N}{2} < N - 1 \end{cases} \quad (24)$$

Further, Eq. (22) is scaled by $\sqrt{2}$ to obtain the resulting signal as

$$x_{ESCO-ACTDT} \approx \begin{cases} x_{even,n}^{cn}, & 0 < n < \frac{N}{2} - 1 \\ x_{even,n}^{|cp|}, & \frac{N}{2} < n + \frac{N}{2} < N - 1 \end{cases} \quad (25)$$

This signal $x_{ESCO-ACTDT}$ is combined with $x_{ATDDT}$ (Eq.(18)) to yield EASCO-DACTDT signal as

$$x_{EASCO-DACTDT} = x_{ATDDT} + x_{ESCO-ACTDT} \quad (26)$$

The demodulation process of received signal $Y_{EASCO-DACTDT}$ is also shown in Fig. 5(b). The enhanced ACO-OFDM (ACO-TDDT) symbols are recovered from $Y_{EASCO-DCTDT\_odd}$ (odd subcarriers of received signal $Y_{EASCO-DCTDT}$).

Following the signal recovery (as described in Section 2.1), the ESCO-ACTDT OFDM symbols are detected from $Y_{EASCO-DACTDT\_even}$ (even subcarriers of received signal $Y_{EASCO-DACTDT}$). As seen in Fig. 5(b), only one FFT is required to demodulate the enhanced ATDDT. For data recovery of ACTDT, an IFFT and two FFT are needed. So, the computational complexity of the receiver is $3\Theta(Nlog_2N)$, which is similar to EASCO-ATDDT and EASCO-ESTDDT system.

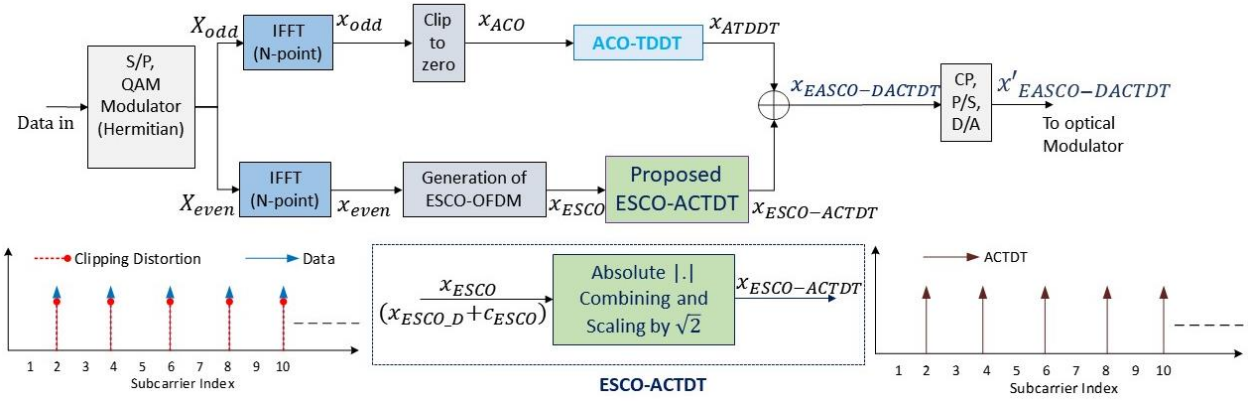


*a*

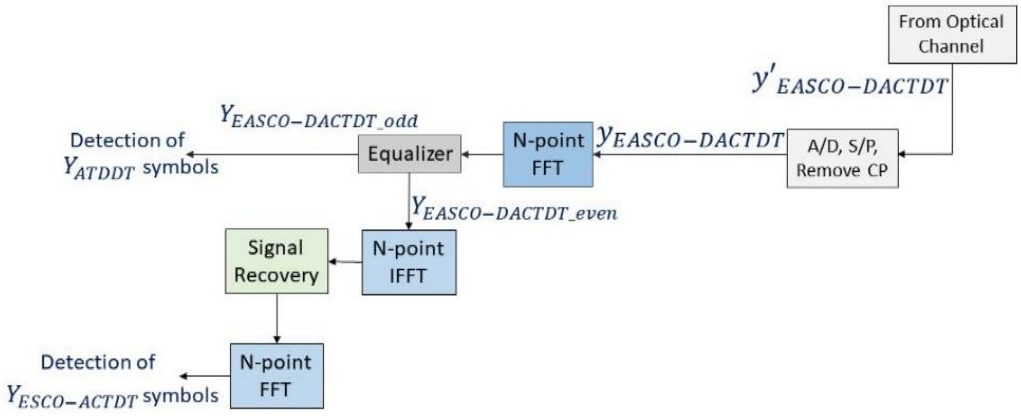


*b*

*Fig. 5. Block Diagram of EASCO-DACTDT OFDM System (a) Transmitter (b) Receiver (color online)*

## 4. Performance analysis

### 4.1. Spectral efficiency analysis

EASCO-ATDDT, EASCO-AESTDDT and the novel EASCO-DACTDT have the same spectral efficiency of EASCO-OFDM. The comparison of spectral efficiencies of ASCO-OFDM, EASCO-OFDM, EASCO-ATDDT, EASCO-AESTDDT and the novel EASCO-DACTDT are listed in Table 2. The spectral efficiencies in Table 2 are for a large $N$ considering the same constellation size and equal optical power for both odd and even subcarriers.

It is evident from Table 2, that variants of EASCO-OFDM, namely EASCO-ATDDT, EASCO-AESTDDT, EASCO-DACTDT OFDM have 33.33% higher spectrally efficiency compared to ASCO-OFDM.

*Table 2. Spectral efficiency comparison*

| Constellation size groups (same on both odd and even subcarriers) | Spectral Efficiency (bits/sec/Hz) | | |
|---|---|---|---|
| | ASCO-OFDM | EASCO-OFDM | EASCO-(ATDDT, AESTDDT, DACTDT) OFDM |
| 4-QAM | 0.75 | 1 | 1 |
| 16-QAM | 1.5 | 2 | 2 |
| 64-QAM | 2.25 | 3 | 3 |
| 256-QAM | 3 | 4 | 4 |
| 1024-QAM | 3.75 | 5 | 5 |

*Table 3. Complexity comparison*

| Optical OFDM systems | Transmitter | Receiver |
|---|---|---|
| ASCO-OFDM | $3\Theta(Nlog_2N)$ | $4\Theta(Nlog_2N)$ |
| EASCO-OFDM | $2\Theta(Nlog_2N)$ | $4\Theta(Nlog_2N)$ |
| EASCO-ATDDT OFDM | $2\Theta(Nlog_2N)$ | $3\Theta(Nlog_2N)$ |
| EASCO-AESTDDT OFDM | $2\Theta(Nlog_2N)$ | $3\Theta(Nlog_2N)$ |
| EASCO-DACTDT OFDM | $2\Theta(Nlog_2N)$ | $3\Theta(Nlog_2N)$ |

### 4.2. Computational complexity comparison

As stated previously in Section 2.2.2, the complexity in this section is also represented by the number of complex multiplications of IFFT/FFT operations. ASCO-OFDM requires two IFFT's to modulate a conventional ACO-OFDM mapping and one IFFT to modulate SCO-OFDM mapping at the transmitter. ASCO-OFDM receiver requires two FFT to demodulate the two frames ASCO-OFDM signal, in addition to an IFFT and a FFT to remove the ACO-OFDM clipping distortion. The computational complexity at the transmitter of ASCO-OFDM is $3\Theta(Nlog_2N)$ and at the receiver is $4\Theta(Nlog_2N)$. In comparison, EASCO-OFDM requires two IFFT's at the transmitter that has a complexity of $2\Theta(Nlog_2N)$. Its receiver requires one FFT to demodulate the signal and an IFFT and FFT to remove the ACO-OFDM clipping distortion. The complexity at the receiver is $4\Theta(Nlog_2N)$. Hence, EASCO-OFDM achieves the reduced complexity at the transmitter when compared to ASCO-OFDM system. EASCO-ATDDT OFDM has a complexity of $2\Theta(Nlog_2N)$ at the transmitter. Since EASCO-ATDDT OFDM receiver does not need the elimination of ACO-OFDM clipping distortion, it requires an FFT to recover the ATDDT-OFDM. It requires one FFT to demodulate the received signal and an IFFT and FFT to recover the ESCO-OFDM symbols. The complexity at the receiver is $3\Theta(Nlog_2N)$.

In addition to IFFT, the TDDT blocks on the ACO-OFDM and ESCO-OFDM stream in EASCO-AESTDDT OFDM requires the linear combining operation at each streams of EASCO-OFDM transmitter that costs $2\times\Theta(N)$. Thus, the overall computational complexity at the transmitter is maintained at $2\Theta(Nlog_2N)$. Similar to ATDDT OFDM receiver, the EASCO-AESTDDT receiver also requires a complexity of $3\Theta(Nlog_2N)$. The EASCO-DACTDT OFDM transmitter similar to EASCO-AESTDDT OFDM has complexity of $2\Theta(Nlog_2N)$. The EASCO-DACTDT OFDM receiver requires three FFT's to demodulate its signals, which has a complexity of $3\Theta(Nlog_2N)$. Computational complexity analysis is summarized in Table 3.

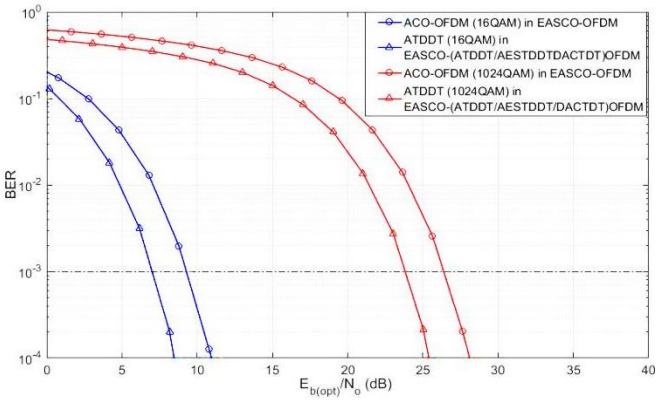


*Fig. 6. BER versus $\frac{E_{b(opt)}}{N_o}$ (dB) for ACO-OFDM and ATDDT-OFDM (color online)*

### 4.3. BER performance

For the BER simulations, the IFFT size *'N'* used is 1024, and an oversampling of 4 was used to improve the accuracy of results. A total of 256 symbols were used. The optical power is also equally allocated to both odd and even streams. For comparison analysis, the BER simulations are carried for the same spectral efficiency of all the models. The method of Equal Gain Combining (EGC) was chosen to achieve the best results for TDDT technique. The BER of ACO-OFDM and ATDDT, which are the odd stream signals of EASCO-OFDM, EASCO-ATDDT, EASCO-AESTDDT and EASCO-DACTDT are compared and analysed in Fig. 6. For 16-QAM, referring to BER of $10^{-3}$, ATDDT has 2.3 dB higher OSNR than the conventional ACO-OFDM. For 1024-QAM, ATDDT performs 2.6 dB better than the conventional ACO-OFDM. The BER performances of ESCO-OFDM, ESTDDT-OFDM and ESCO-ACTDT OFDM, which are the even stream signals of EASCO-OFDM, EASCO-ATDDT, EASCO-AESTDDT and EASCO-DACTDT are compared and analysed in Fig. 7.

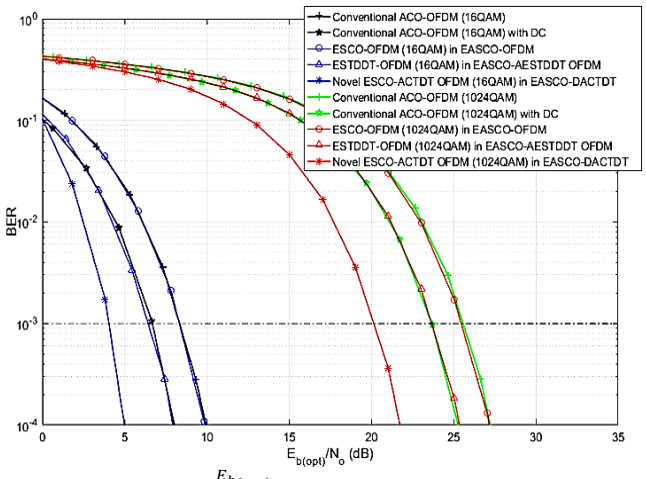


*Fig. 7. BER versus $\frac{E_{b(opt)}}{N_o}$ (dB) for ESCO-OFDM, ESTDDT-OFDM and ESCO-ACTDT OFDM (color online)*

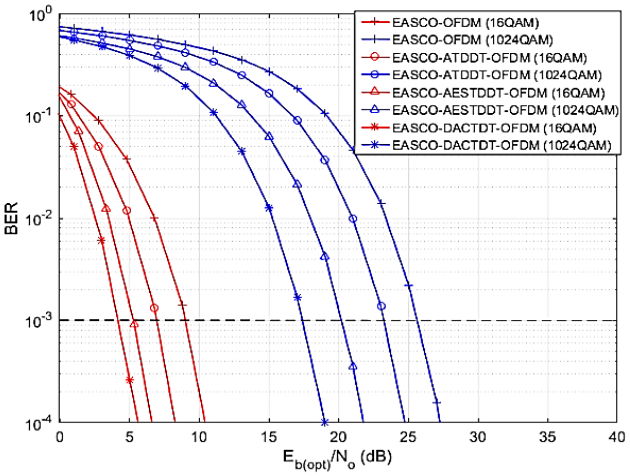


*Fig. 8. BER versus $\frac{E_{b(opt)}}{N_o}$ (dB) for EASCO-OFDM, EASCO-ATDDT OFDM, EASCO-AESTDT OFDM and the novel EASCO-DACTDT OFDM (color online)*

The BER performance of ESTDDT-OFDM and ESCO-OFDM is the same as the conventional ACO-OFDM with and without DC respectively. For 16-QAM and BER of $10^{-3}$, the novel ESCO-ACTDT has 2 dB higher OSNR than ESTDDT-OFDM and 4.3 dB better than the ESCO-OFDM. For 1024-QAM, ESCO-ACTDT performs 1.8 dB better than ESTDDT-OFDM and 5.3 dB better than the ESCO-OFDM. Thus, efficient utilization of the clipping distortion of ESCO-OFDM and reduced noise effect by the proposed ESCO-ACTDT results in better performance when compared to ESTDDT-OFDM and the conventional ACO-OFDM with TDDT. When the data is clipped on the even subcarriers, ACTDT technique can be effectively applied to achieve better utilization of the clipping distortion at a reduced receiver complexity than the conventional TDDT.

The BER of EASCO-AESTDDT OFDM is compared with EASCO-OFDM, EASCO-ATDDT and the novel EASCO-DACTDT OFDM, which is shown in Fig. 8. As seen in Fig. 8, in terms of Optical Signal-to-Noise Ratio, $\frac{E_{b(opt)}}{N_o}$ (OSNR), for 16-QAM and BER of $10^{-3}$, EASCO-ATDDT OFDM (TDDT applied only to ACO-OFDM signal) performs 1.2 dB better than EASCO-OFDM. For 1024-QAM, EASCO-ATDDT OFDM performs 2.7 dB better than EASCO-OFDM. For 16-QAM and BER of $10^{-3}$, EASCO-AESTDDT with enhanced receiver (TDDT applied to both stream of (ACO and ESCO)-OFDM respectively) performs 1.7 dB better than EASCO-ATDDT and 2.9 dB better than EASCO-OFDM. For 1024-QAM and BER of $10^{-3}$, EASCO-AESTDDT performs 3 dB better than EASCO-ATDDT and 5.8 dB better than EASCO-OFDM.

For 16-QAM, the novel EASCO-DACTDT OFDM performs 2 dB better than EASCO-AESTDDT OFDM, 3.6 dB better than EASCO-ATDDT, and 4.8 dB better than EASCO-OFDM. For 1024-QAM, novel EASCO-DACTDT OFDM performs 2.4 dB better than EASCO-AESTDDT OFDM and 5.5 dB better than EASCO-ATDDT OFDM and 8.3 dB better than EASCO-OFDM.

## 5. Conclusion

A novel EASCO-DACTDT OFDM system is presented. This technique improves the BER with reduced complexity in comparison to the conventional technique. This paper presents the transceiver designs of proposed EASCO-DACTDT OFDM together with its intermediate systems called the EASCO-ATDDT and EASCO-AESTDDT. The performances were analysed in terms of spectral efficiency, computational complexity and BER. The optical power allocations, Error vector magnitude (EVM) and peak average to power ratio (PAPR) and the nonlinearity of the LEDs will be investigated in the future work.

### Acknowledgments

The authors extend their appreciation to the Deanship of Scientific Research at King Saud University for funding this work through Research Group No. RG-1439-004.

## References


[1] S. D. Mohamed, H. M. Shalaby, I. Andonovic et al., Optics Communications **380**, 61 (2016).

[2] B. Ranjha, M. Kavehrad, IEEE/OSA Journal of Optical Communications and Networking **6**(4), 387 (2014).

[3] A. J. Lowery, Optics Express **24**(4), 3950 (2016).

[4] Q. Wang, C. Qian, X. Guo et al., Optics Express **23**(9), 12382 (2015).

[5] S. D. Dissanayake, J. Armstrong, Journal of Lightwave Technology **31**(7), 1063 (2013).

[6] S. D. Dissanayake, K. Panta, J. Armstrong, in 2011 IEEE GLOBECOM Workshops (GC Wkshps), 782-786, IEEE (2011).

[7] M. S. Baig, A. F. Abas, M. T. Alresheedi, in IEEE 2017 8th International Conference on Information Technology (ICIT), 785-789, IEEE (2017).

[8] J. Xu, W. Xu, H. Zhang et al., IEEE Photonics Journal **8**(1), 1 (2016).

[9] E. Katz, A. Laufer, Y. Bar-Ness, IEEE 46th Annual Conference on Information Sciences and Systems (CISS), 1-6 (2012).

[10] L. Chen, B. Krongold, J. Evans, GLOBECOM, IEEE Global Telecommunications Conference 1-6, IEEE (2009).

[11] N. Wu, Y. Bar-Ness, In IEEE 2014 48th Asilomar Conference on Signals, Systems and Computers, (ACSSC) 1381-1386, IEEE (2015).

[12] M. M. Mohammed, C. He, J. Armstrong, Journal of Lightwave Technology **35**(11), 2078 (2017).

[13] J. Li, X. Liu, J. Li et al., Optics Communications, **443**, 86 (2019).

[14] N. Wu, Y. Bar-Ness, EURASIP Journal on Advances in Signal Processing **2015**(1), 1 (2015).

[15] E. Lam, S. K. Wilson, H. Elgala et al., arXiv preprint arXiv:1510.08172, (2015).

[16] R. Bai, Q. Wang, Z. Wang, Journal of Lightwave Technology **35**(17), 3680 (2017).

[17] M. S. Islim, H. Haas, Optics Express **24**(11), 11932 (2016).

[18] Q. Wang, Z. Wang, L. Dai, Journal of Lightwave Technology **32**(22), 3869 (2014).



*Corresponding author: aabas@ksu.edu.sa